

Improving B_1^+ Uniformity Using Segmented Dielectric Pads

Aurelien Destrue¹, Jin Jin¹, Feng Liu¹, Mingyan Li¹, Ewald Weber¹, and Stuart Crozier¹
¹School of ITEE, University of Queensland, Brisbane, Queensland, Australia

TARGET AUDIENCE: Engineers and researchers interested in understanding and designing dielectric pads for high field MRI.

INTRODUCTION: It has been shown that high-permittivity dielectric pads can be used to efficiently improve the B_1 field homogeneity in the region of interest (ROI) in high-field MRI [1-8]. Recent studies focused on the design of these pads by controlling parameters such as size, position and permittivity, using simple patient specific parameter sweeping to improve the transmit field in a small region. In most cases, two pads with identical permittivities are placed on the opposite sides of the ROI (left/right for brain imaging, front/back for chest imaging). In these cases, the dimensions of the pads are similar to that of the ROI [1-4]. In this study, we analyse the fundamental behaviour of the dielectric pads and demonstrate how segmenting bigger pads into smaller ones with different permittivities can significantly improve the dielectric shimming.

METHODS: The positioning of the pads in the literature is intuitive, as these pads can be considered as secondary sources of magnetic field H , according to Maxwell's equation :

$$\nabla \times H = J_c + J_d = \sigma E + i\epsilon_r \epsilon_0 \omega E \quad (1)$$

where J_c and J_d are the conductive and displacement currents, E is the electric field, σ is the conductivity, ϵ_r is the relative electric permittivity, ϵ_0 is the electric permittivity in vacuum, ω is the angular frequency and i is the imaginary unit. Because of their dielectric property ($\sigma \ll \epsilon_r$), the field generated by high-permittivity pads is primarily induced by the displacement currents, which are proportional to the volume and permittivity of the pads [1, 6-8].

In this study, two conventional dielectric shimming approaches are evaluated, namely the local shimming and global shimming. Figure 2A illustrates the local shimming strategy, where two pads are positioned close to the B_1^+ drop-off regions. Figure 2B shows the global shimming approach, where a single pad is wrapped around the subject. We propose a novel approach where larger pads are segmented into narrower ones in order to constrain the displacement current to the Z-direction (Figure 2C). Since the displacement currents are also related to the permittivity, we additionally investigated whether allowing the segmented pads to have different permittivities can further improve the B_1^+ homogeneity (Figure 2D). These new approaches are compared with the conventional approaches, focusing on 7T head imaging.

A head-sized uniform elliptic cylindrical phantom of average head tissue at 7T ($\epsilon_r = 36$, $\sigma = 0.65$ S/m) was modelled in FEKO (EMSS, SA). Eight rectangular loop coils equally distributed around the subject in the angular direction were excited in the circular polarization mode. In all the configurations, the thickness of the pads was set to 10 mm and the height to that of the phantom. The conductivity of the pads was kept at 0, and their permittivities were limited to $\epsilon_r = 250, 300$ or 350 . B_1^+ homogeneity in the centre slice (ratio between standard deviation and mean, the lower the better) was calculated for the four approaches and compared to the case without pads (Figure 1). In approach A, B and C, the permittivity was kept constant between sections, but varied in different simulations to determine the best ϵ_r . In approach D, all combinations of ϵ_{r1} , ϵ_{r2} , ϵ_{r3} and ϵ_{r4} were evaluated.

RESULTS AND DISCUSSION: In Figure 2A, the best transmit uniformity is obtained with $\epsilon_r = 300$. In this case, the correlation between magnitude of surface current and gain of B_1^+ , expected from Eq 1, is not observed. Although the strength of the field is greatly improved in regions close to the pads, the overall transmit uniformity is degraded. Approach B, with $\epsilon_r = 250$, demonstrated a significant improvement of 40% from the case without pad. However, it can be seen in Figure 2B (top) that the displacement currents occur all around the pad at a much higher magnitude, but with no clear relationship with B_1^+ . An explanation can be found in Figure 3A, which demonstrates that in these cases most of the currents flow in the XY-plane, and thus do not contribute to the improvement of transverse magnetic field. For this reason, in approach C the large pad is split into eight narrower pads to limit the displacement currents between regions, thereby decreasing the currents in the angular direction. It is shown in Figure 3B that currents are much weaker in the XY-plane and enhanced in the Z-direction. Figure 2C shows that although the direction of the displacement current was more suited to improve the uniformity of the transverse magnetic field, its distribution around the phantom was not optimal. In addition to changing the direction of the displacement currents, splitting the pads provided increased degrees-of-freedom in dielectric shimming, as each pad can have a different permittivity. Every combination of available permittivities was evaluated, and Figure 2D illustrates the best transmit uniformity achieved with the combination $\epsilon_{r1} = 250$, $\epsilon_{r2} = 300$, $\epsilon_{r3} = 350$ and $\epsilon_{r4} = 300$, with an improvement of 47% compared to the case without pad. It can be expected that having even narrower pads in greater number and more available permittivities may further improve the effectiveness of the dielectric shimming.

CONCLUSION: In this work, the displacement current in high-permittivity dielectric pads was analysed and a new perspective was introduced in designing dielectric shim. We noticed that besides increasing the volume or permittivity of the pads, it is important to optimise their geometries in favour of displacement currents participating in the improvement of the B_1^+ field. Furthermore, introducing multiple pads with different permittivities offers more degrees-of-freedom to control the overall distribution of displacement current, and thus the uniformity of B_1^+ . Future work will investigate the possibility of efficiently modelling the displacement currents, as a way to accelerate the computing time for pad optimization. The method will also be implemented on realistic human models and validated by experiments.

REFERENCES: [1] Brink et al., *MRM* 2014, 71:1632-1640; [2] Teeuwisse et al., *MRM* 2012, 67:1285-1293; [3] Teeuwisse et al., *MRM* 2012, 67:912-918; [4] Brink et al., *Invest. Radio*. 2014, 49:271-277; [5] Yang et al., *J MRI* 2013, 38:435-440; [6] Yang et al., *MRM* 2011, 65:358-362; [7] Yang et al., *J MRI* 2006, 24:197-202; [8] Webb, *Concepts in MR* 2011, 38:148-184;

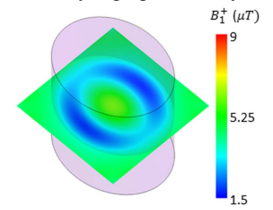


Figure 1. Simulated B_1^+ in the centre slice of the elliptic phantom, without dielectric pad.

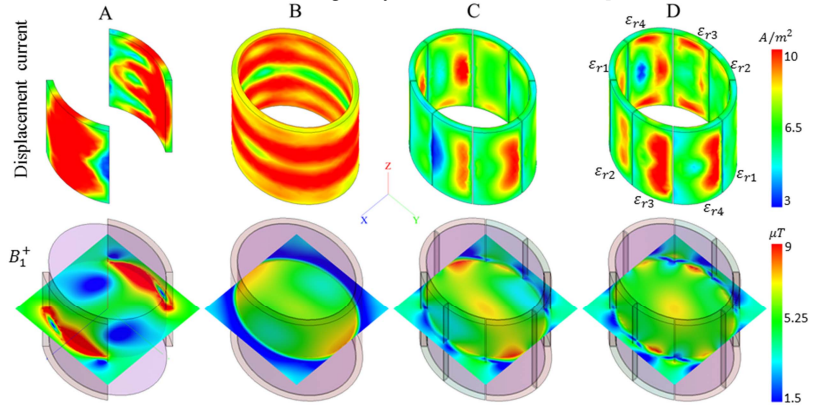


Figure 2. Displacement current (top row) and B_1^+ in the center slice (bottom row) in the different configurations of dielectric pads investigated. (A) Two Pads placed close to the B_1^+ drop-off, (B) a single pad wrapped around the phantom, (C) Eight pads distributed around the phantom with equal permittivities, (D) Eight pads with independent permittivities, making use of the central symmetry of the displacement current distribution.

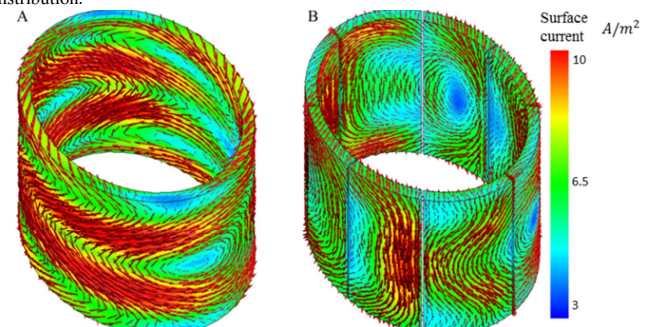


Figure 3. Instantaneous magnitude of the surface current in a single pad (A) and in eight pads with same ϵ_r (B).